NASA TECHNICAL
MEMORANDUM

NASA TM X-53857

ACCELEROMETER CALIBRATION IN THE LOW g RANGE BY MEANS OF MASS ATTRACTION

By Konrad Reinel
Astrionics Laboratory

July 28, 1969

NASA

George C. Marshall Space Flight Center
Marshall Space Flight Center, Alabama

1. REPORT NO. TM X-53857	2. GOVERNMENT ACCESSION NO.	3. RECIPIENT'S CATALOG NO.
4. TITLE AND SUBTITLE Accelerometer Calibration in the Low g Range by Means of Mass Attraction		5. REPORT DATE July 28, 1969
		6. PERFORMING ORGANIZATION CODE
7. AUTHOR(S) Konrad Reinel		8. PERFORMING ORGANIZATION REPORT #
9. PERFORMING ORGANIZATION NAME AND ADDRESS George C. Marshall Space Flight Center Marshall Space Flight Center, Alabama 35812		10. WORK UNIT NO.
		11. CONTRACT OR GRANT NO.
12. SPONSORING AGENCY NAME AND ADDRESS		13. TYPE OF REPORT & PERIOD COVERED Technical Memorandum
		14. SPONSORING AGENCY CODE
15. SUPPLEMENTARY NOTES Prepared by Astrionics Laboratory, Science and Engineering Directorate		

16. ABSTRACT

   Mass attraction is used as an equivalent acceleration input to calibrate an accelerometer. The upper limit of the acceleration by a reasonable mass size is 10^{-9} g in orbit and 10^{-7} g in the laboratory.   The calibration has been carried out in the laboratory for an electrostatic suspended single-axis accelerometer (MESA) with a variable mass attraction.   The mass attraction input to the accelerometer was a sine wave with the amplitude of 23 nano g.   The response of the accelerometer to this acceleration input by mass attraction was obtained by data analysis and data reduction with a computer.   The results of the experiment agree with the scale factor of the accelerometer for higher acceleration inputs.   Application of the mass attraction principle as a calibration method of accelerometers for very low accelerations (for instance, in orbit) is proposed.

17. KEY WORDS Low g accelerometer Mass attraction testing MESA accelerometer testing	18. DISTRIBUTION STATEMENT Announce in STAR		
19. SECURITY CLASSIF. (of this report) Unclassified	20. SECURITY CLASSIF. (of this page) Unclassified	21. NO. OF PAGES 46	22. PRICE $3.00

MSFC - Form 3292 (May 1969)

ACKNOWLEDGMENTS

TABLE OF CONTENTS

LIST OF FIGURES

LIST OF FIGURES (Concluded)

LIST OF TABLES

DEFINITION OF SYMBOLS

Symbol	Definition
g	Earth attraction $981.0 \frac{cm}{s^2}$
μg	Micro g = 10^{-6} g
ng	Nano g = 10^{-9} g
X, Y, Z	Cartesian coordinates of the attracting mass
M	Attracting mass
m	Proof mass of the accelerometer
F	Force of mass attraction
γ	Universal gravitational constant
R	Distance between two mass points
A	Acceleration by mass attraction
A(I)	Variable acceleration input
X	Direction of the accelerometer input axis
r	Radius of a sphere
ρ	Density
d	Distance between center of proof mass m and surface of attracting mass M
k	Length of a lead cube
E	Error of replacing the cubes by mass points
NA	Amplitude of the acceleration input

DEFINITION OF SYMBOLS (Continued)

Symbol	Definition
I	Measurement number
MESA	Miniature electrostatic accelerometer
AX(I)	MESA data
AY(I)	Tilt meter data
X(I)	MESA data with zero mean value
Y(I)	Tilt meter data with zero mean value
PSD	Power spectral density
A(K)	Fourier coefficient
B(K)	Fourier coefficient
K	Harmonic number
XSM(I)	Mean value of X(I) between I−JA and I+JA
RX(L)	Autocorrelation function of X(I)
L	Lag number
F(K)	Frequency of the Kth harmonic
G(K)	PSD amplitude of the random and periodic data
GR(K)	PSD amplitude of the random data
GO(K)	PSD amplitude of the periodic data
CR(K)	Fourier amplitude for the Kth harmonic
XSD	Standard deviation of X(I)

DEFINITION OF SYMBOLS (Concluded)

Symbol	Definition
AM	Mean value of the accelerometer response to the input
SC	Scale factor of MESA
XM, YM	Mean value of AX(I) and AY(I), respectively
N	Number of measurements
FN	Nyquist frequency
H	Sampling time
FO	Frequency of the acceleration input caused by mass attraction
RXY(L)	Cross-correlation function of X(I) with Y(I)
GS(K)	Power spectral density function
ML	Maximum lag number
P	Multiplication factor of the tilt meter data
XR(I)	Data X(I) after reduction

ACCELEROMETER CALIBRATION
IN THE LOW g RANGE
BY MEANS OF MASS ATTRACTION

SUMMARY

Mass attraction is used as an equivalent acceleration input to calibrate an accelerometer. The upper limit of the acceleration by a reasonable mass size is 10^{-9} g in orbit and 10^{-7} g in the laboratory. The calibration has been carried out in the laboratory for an electrostatic suspended single-axis accelerometer (MESA) with a variable mass attraction. The mass attraction input to the accelerometer was a sine wave with the amplitude of 23 nano g. The response of the accelerometer to this acceleration input by mass attraction was obtained by data analysis and data reduction with a computer. The results of the experiment agree with the scale factor of the accelerometer for higher acceleration inputs. Application of the mass attraction principle as a calibration method of accelerometers for very low accelerations (for instance, in orbit) is proposed.

INTRODUCTION

Generally, the single-axis accelerometer, used for inertial navigation, is tilted in the earth's gravitational field for its calibration between ±1 g and ±1 μg, where the acting acceleration is a function of the angle between the sensitive accelerometer axis and the local vertical. The input axis is almost horizontal for low g calibration, and the accuracy of this method is limited by the measurement of a very small angle. The resolution of the best available theodolite is 0.1 arc sec with an accuracy of 0.2 arc sec. The angle of 0.2 arc sec limits the calibration accuracy to 1.0 μg. This is sufficient for almost every inertial navigation system. An acceleration error of 1.0 μg in an inertial navigation system would cause a position error of 50 m after 1 hour.

However, some necessary measurements in space require a calibration of the accelerometer far beyond this 1-μg limit. The Apollo Application Program includes the measurement of the gravity gradient anomalies of the moon from a satellite [1]. Gravity gradient is a function of mass distribution, and every

mass concentration near the surface of the moon will generate a deviation of the measured gravity gradient from the calculated gravity gradient of a homogeneous sphere. These gravity gradient anomalies of the moon are expected to be very large because of the big mass concentrations (mascons), which have already been detected by the lunar orbiter data [2]. The gravity gradient of the moon in the proposed 55-km orbit is about 2×10^3 Eoetvoes units. The required performance of the experiment is to measure 0.5 Eoetvoes units to determine the magnitude and direction of the lunar gravity gradient anomalies. One Eoetvoes unit is $10^{-9} \frac{1}{\sec^2}$ or $1.018 \times 10^{-12} \frac{g}{cm}$. If an accelerometer is used as a gravity gradient sensor at a 2-m distance from the mass center of the satellite, the required threshold is 10^{-10} g.

The accelerometer must be tested and calibrated for this low g application. Because a range of just 10^{-6} g is in the state of the art, the accelerometer must be switched in the orbit to this high sensitive range after the large acceleration of the launch.

An attempt has been made to calibrate an accelerometer in earth orbit with a centrifuge [3]. (This calibration was limited to 10^{-6} g.) The apparent acceleration is a function of the distance from the rotation center and of the angular velocity. The angular velocity would be as small as $10^{-3} \frac{rad}{\sec}$ for a 10^{-9}-g acceleration of a mass point at a 2.5-cm distance from the rotation center. It would be very difficult to get such a low constant angular velocity in the satellite.

This paper describes the use of the mass attraction of a rigid body for the calibration of an accelerometer in the range below 10^{-9} g in a satellite and below 10^{-7} g in the laboratory. The size of the mass that can be handled is the limiting factor.

Calibration in the laboratory with the mass attraction method has been carried out and is described. A proposal is made for the calibration of an accelerometer in a satellite.

MASS ATTRACTION AS CALIBRATION FORCE

Generally, a component of the mass attraction force between the accelerometer and the earth is used for calibration, but, for the low g range, the mass attraction of a smaller rigid body has some advantage because the

2

acting acceleration is a function of the size of the mass. It is very easy to generate a small acceleration by mass attraction, but there are two problems: The accelerometer must be able to sense this small acceleration, and the system must often separate this small input acceleration from much larger background disturbances.

The lower limit of acceleration sensing is given by the threshold of the accelerometer and the requirements for the experiment. The upper limit is given by the size of the mass. Because the mass must change its position to generate a variable additional acceleration input, the mass should be of a size that can be handled. The mass used in the laboratory experiments was about 1000 kg; in a satellite, it might be about 1 kg. Therefore, the corresponding limits of the mass attraction are about 0.05 μg in the laboratory and 0.001 μg in the satellite.

The disturbances in the laboratory are the unknown tilt angle of the accelerometer in the earth field, tilting of the foundation, bending of the fixture, and changing of the temperature; the disturbances in a satellite are mass attraction of some other parts of the satellite, changing of the temperature, and acceleration by gravity gradient of the orbited planet. Because generally these disturbances cannot be eliminated, they are separated by filtering as discussed in this paper. The input acceleration is changed with a certain frequency, which should not correspond with the frequency of any other acceleration. The input frequency of the mass attraction can be very low. The variation of the mass attraction is either a change in the distance between the accelerometer and the attracting mass or a change in the angle between the sensitive accelerometer axis and the vector of the mass attraction.

The response of the accelerometer to the mass attraction force can be obtained by a conventional data analysis utilizing a computer.

MASS ATTRACTION OF A RIGID BODY

The accelerometer to be calibrated is a single-axis device; therefore, only the acceleration component along the input axis is of interest. The proof mass of the accelerometer is m and the calibrating large mass is M. The Cartesian coordinate system X, Y, Z has its origin at the center of m and its X-axis along the sensitive axis of the accelerometer (Fig. 1).

If m and M are two mass points with the positions (0,0,0) and (X, Y, Z), the attraction force F in the X direction would be [4]

Figure 1. Attraction of two mass points.
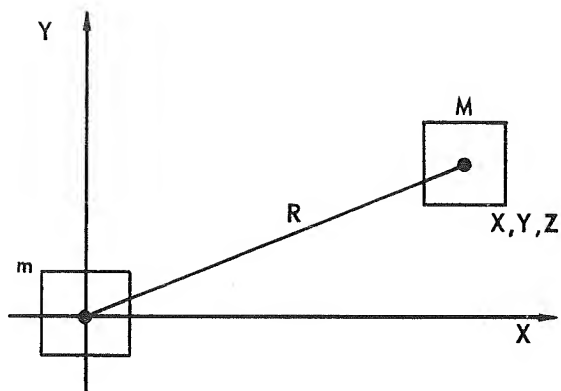
$$F_X = \gamma \frac{m \times M \times X}{R^3} \qquad (1)$$

$$\gamma = 6.67 \times 10^{-8} cm^3 gm^{-1} s^{-2}$$

$$R = (X^2 + Y^2 + Z^2)^{\frac{1}{2}}$$

m = proof mass

M = attracting mass;

γ is the universal gravitational constant in CGS units, and R is the distance between the mass points. The acceleration A of the proof mass along the input (X) axis is

$$A = \gamma \, M \, \frac{X}{R^3} \qquad . \qquad (2)$$

This equation is also correct if the calibrating mass M is an extended homogeneous sphere. Then R is a sum of the radius r of the sphere and the distance d between the center of the proof mass and the surface of the sphere; r changes with the mass M. The acceleration of a lead sphere on the X-axis with a density of $\rho = 11.34 \frac{gm}{cm^3}$ in a distance of d = 10.2 cm from the proof mass is shown in Table 1. For an acceleration of 10^{-7} g the mass would weigh 4700 kg. This is already too much to handle easily in a laboratory.

TABLE 1. ACCELERATION BY A LEAD SPHERE

Mass (kg)	Acceleration (g earth)	Radius of the Sphere (cm)
0.15	10^{-10}	1.5
4	10^{-9}	4.4
68	10^{-8}	11.25
4700	10^{-7}	46.3
1.4×10^6	10^{-6}	307
1.4×10^{24}	1	3.07×10^8

The mass attraction of a rigid body with an irregular shape is given by a triple integral and has no general analytical solution; but if the distance between the proof mass and the rigid body is large in relation to the size of the body, then the attraction is the same as that of a sphere or a mass point with the mass M [5]. Therefore, the mass M was considered to be cut into small cubes of the dimension k with an imaginary point mass M_i in the center of each cube (Fig. 2). The mass attraction is computed for every cube and the sum of all cubes is the attraction of the whole body.
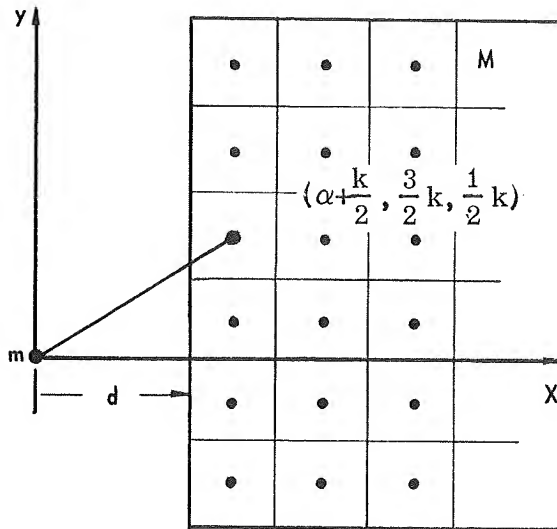
Figure 2. Attraction of a large body.

Figure 3. Error for the approximation of a cube by a mass point.

The quality of this approximation is shown in Figure 3. The error E is a function of the ratio of the distance R to the length k of the cube,

$$E = 1 - \frac{A \text{ (cube)}}{A \text{ (point)}}$$

(dimensionless) . (3)

For a 10^{-3} accuracy of the approximation of a cube by a mass point, the cube length k should be less than one-half the smallest distance. In the experiment, the distance between the center of the nearest cube and the center of the proof mass was 10.2 cm. The length of the cube was 5.1 cm.

In the computation of the mass attraction, the cylindrical proof mass of the MESA was also considered as a mass point. The error of this approximation is less than 10^{-3} for all cubes.

The attracting mass was limited to less than 1500 kg by the available suspension capability. Therefore, an optimization was made by changing the shape of the mass. The mass attraction for every possible cube in a space of 20k by 20k by 10k was calculated. The first 900 most attracting cube locations were chosen for the attracting mass of the experiment. Figure 4 shows the
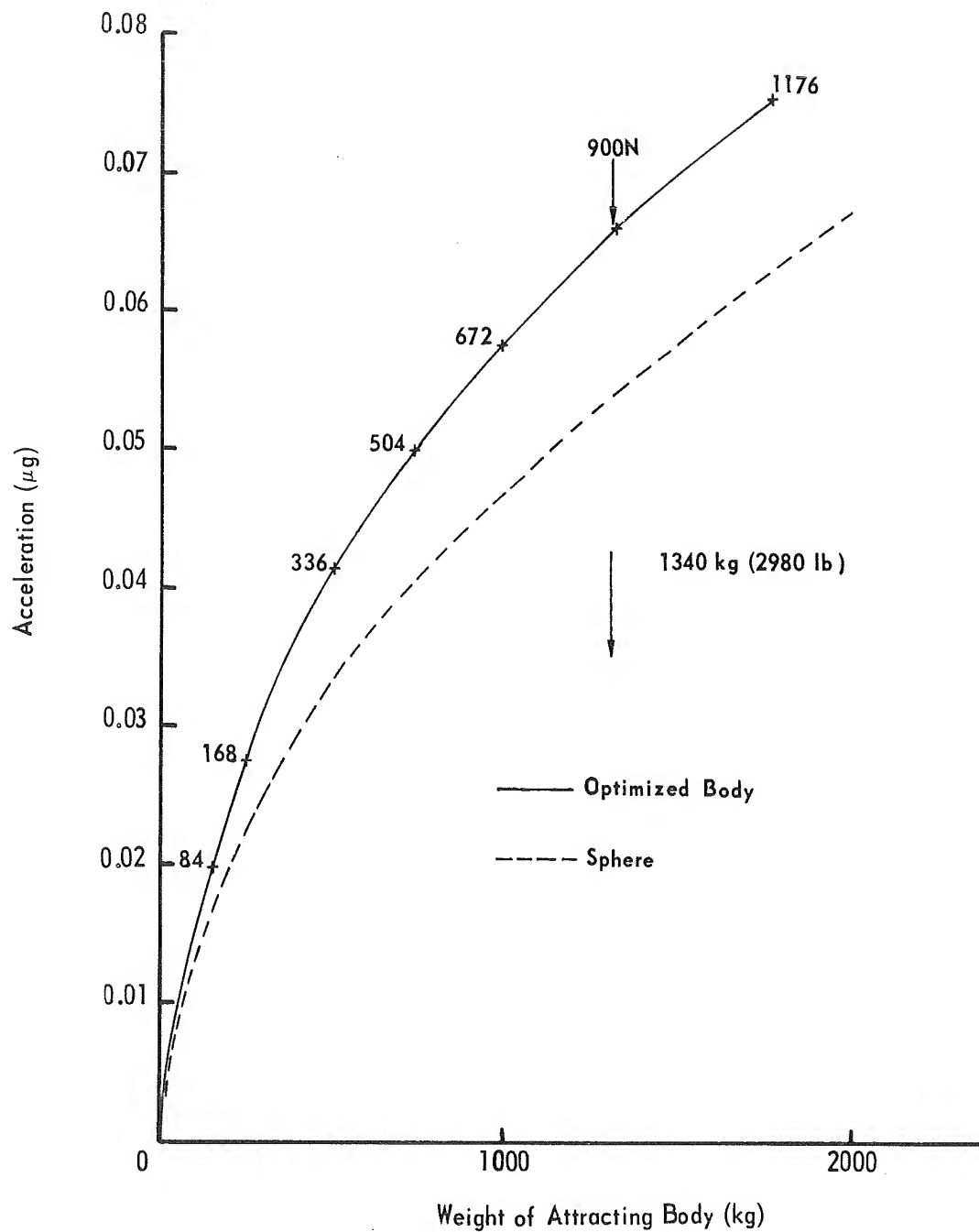
Figure 4. Optimization of the attracting mass.

relation between a sphere and an optimized body during assembly. The distance d between the proof mass center and the surface of the attracting body was 10.2 cm in this graph.

The input acceleration is varied by changing the distance d between the proof mass and the surface of the attracting body (Table 2). The body that was used is a compound of 100 lead cubes with 10.2-cm lengths each and 100 lead cubes with 5.1-cm lengths each. To get a change in the attraction of 70 ng, the mass must be moved about 76.2-cm along the input axis of the accelerometer.

TABLE 2. ATTRACTION OF THE PROOF MASS BY THE LEAD BODY

Distance d (cm)	Mass Attraction (ng)
5.1	81.8
10.2	67.2
12.7	60.8
25.4	38.1
38.1	25.3
50.8	17.7
63.5	13.0
76.2	10.0

CALIBRATION IN THE LABORATORY

Experiment Setup

The maximum acceleration produced by a mass less than 1500 kg is not more than 75 ng for a nearest distance of 7.6 cm between the center of the accelerometer proof mass and the surface of the attracting mass. The same amount of acceleration would appear by an input axis tilt of 0.015 arc sec into the gravity vector. The uncontrolled movement in the laboratory of people stepping on the test pad causes disturbances much larger than 0.1 μg; therefore, almost every experiment was made after working time when the test room was locked. But even then, the tilting of the test pad was measured with an accurate tilt meter during the experiments.

The maximum change of 75 ng could not be obtained in the laboratory because the necessary movement of the lead mass was impossible. The movement of the lead mass on the floor would cause some additional tilting of the test pad. Therefore, a suspension of the mass on an I-beam of the ceiling was considered best. But in this case, the colinear movement of the mass along the horizontally aligned accelerometer input axis would require too large a force pulling horizontally. The chosen change of the mass attraction along the accelerometer input axis was a movement along the vertical.

The vertical movement changed the acceleration component along the input axis because the angle between the input axis and the mass attraction vector was varied. The lead mass was lowered and raised with an electrical hoist. The acceleration of the accelerometer proof mass caused by the mass attraction of the lead body is shown in Table 3 for different vertical positions. The distance between the center of the accelerometer float and the surface of the attracting lead body, in the zero position, is 7.6 cm. Figure 5 is a drawing of the experimental setup for the calibration of the accelerometer using this mass attraction scheme.

TABLE 3. ACCELERATION OF THE ACCELEROMETER FLOAT BY THE LEAD BODY FOR DIFFERENT VERTICAL POSITIONS

Vertical Position (cm)	Acceleration (ng)	Vertical Position (cm)	Acceleration (ng)
0	74.017	27.9	45.979
2.5	73.469	30.5	41.127
5.1	72.559	33.1	36.372
7.6	71.280	35.6	31.954
10.2	69.623	38.1	28.003
12.7	67.571	40.7	24.548
15.2	65.103	43.2	21.562
17.8	62.196	45.7	18.904
20.3	58.823	48.2	16.788
22.9	54.970	50.7	14.890
25.4	50.658	53.3	13.254

The experimental setup allowed a total vertical travel of just 30.5 cm. To get the maximum change in the mass attraction, an optimization study was made. It showed that if the mass is moved vertically between 12.7 cm and 43.2 cm below the zero position, the change in acceleration is maximized.
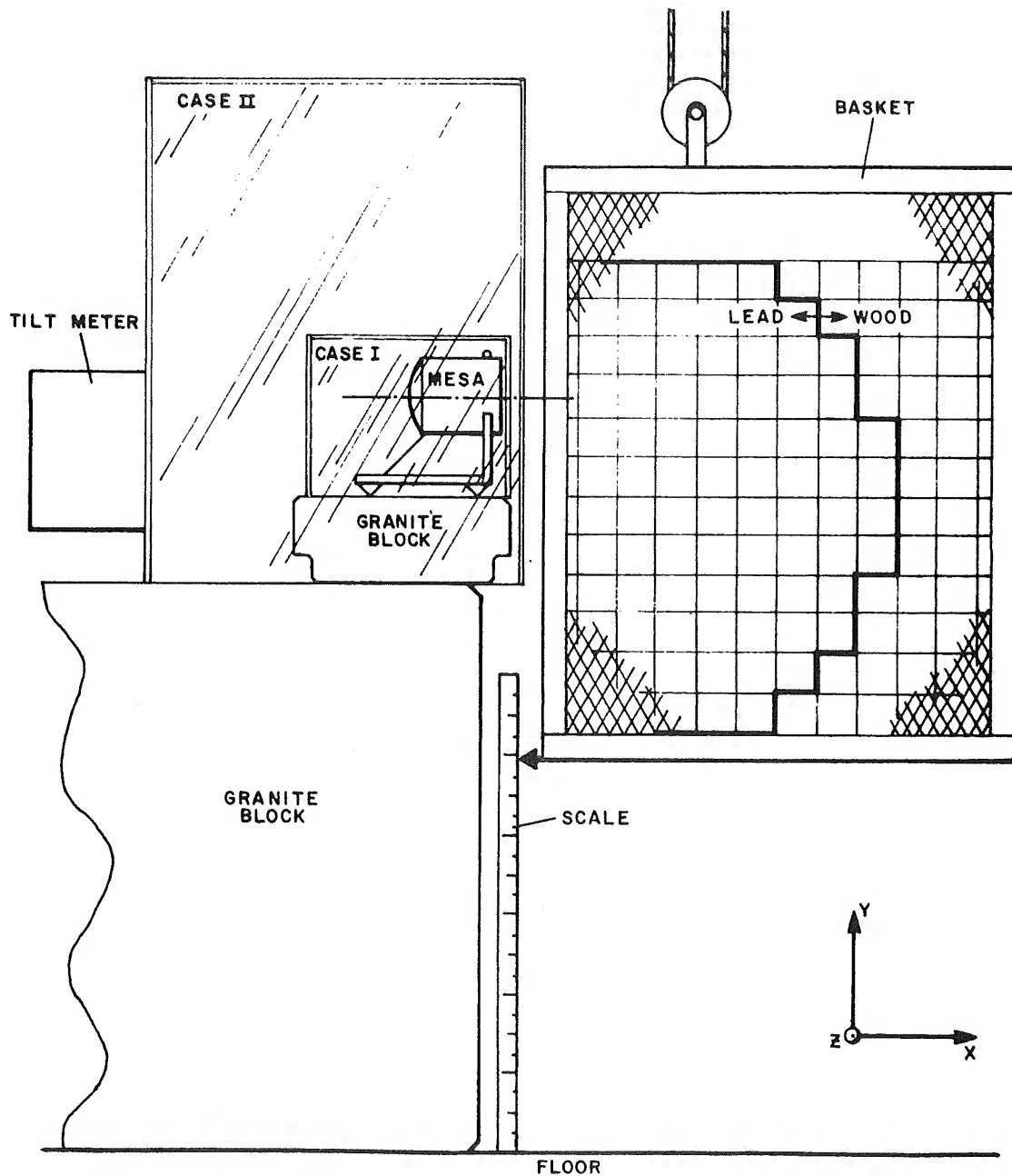
Figure 5. Test setup for the calibration of the miniature electrostatic accelerometer in the laboratory.

For the harmonic determination, the input acceleration for as few as four points of a sine wave of vertical position were recorded: middle, maximum, middle, minimum. The maximum position was at a vertical distance of

12.7 cm below the zero position, the minimum position was 43.2 cm below and the middle position was 28.6 cm below. The middle position was chosen so that the input acceleration at that position is the average of that occurring at maximum and minimum positions. The succeeding run through these positions produces a sine-wave input A(I) with an amplitude NA

$$NA = (23.0 \pm 0.2)\ 10^{-9}g \qquad A(I) = NA \sin\left(\frac{\pi}{2} I\right) \qquad .$$

With a movement larger than 100 cm, the input amplitude could be as high as 0.037 μg with the same mass and the same components.

To demonstrate low g accelerometer calibration, the MESA, manufactured by Bell Aerosystems, was used [6]. The MESA is a single-degree-of-freedom accelerometer with an electrostatically suspended proof mass. This proof mass is a thin-walled beryllium cylinder with a flange for pickoff and restraint. The cylinder length is 2.915 cm and the inner diameter is 1.268 cm. The distance between the center of the float and the mounting surface of the accelerometer is 3.134 to 3.190 cm.

The proof mass suspension force is adjustable to correspond to different accelerations of the environment. A pulsed force rebalance technique is used to constrain the proof mass along its sensitive axis. The pulse rate is proportional to the acceleration along the cylinder axis (input axis). The MESA that was used had two ranges: low g range with 10.21 pps/μg and high g range with 1.024 pps/μg. For the whole experiment, the MESA was used in the low g range. The technical data in the acceptance test of the MESA in the low g range are

null stability = 0.163×10^{-6} g (4-hour period)

scale factor stability = $\pm 0.01758\%$ ($\pm 0.1\%$ – 4 hours)   .

The mounting of the MESA is a clamp type around the case to get a small distance between the MESA and the lead surface.

A tilt meter made by Ideal Aerosmith was set on the same test pad to measure tilts of the foundation [7]. The surfaces of two interconnected mercury pools 1 m apart serve together with two rigidly mounted plates as two capacitors. Any tilting will change the capacities, which can be expressed in tilt angles. The tilt meter was used in the high range. The output of the null meter was calibrated so that a tilt of 0.0067 arc sec produced a voltage

of 0.1V. This voltage was fed to an integrating digital voltmeter. Both the accelerometer data and the tilt meter data were automatically punched on a paper tape for computer use.

The attracting mass, 100 lead cubes of 10.2 cm lengths and 100 lead cubes of 5.1-cm lengths, was assembled in the optimized shape (Fig. 6). The free spaces in the basket were filled with the same size of wooden cubes.

The time for every measurement was H=100 seconds. This large measuring time was necessary to get a minimum number of impulses required for statistical data handling. During the measurement, the mass remained in position. At the end of one measurement, the mass was raised or lowered to the next position. The time between the measurements was always 20 seconds. In every series, at least 100 measurements corresponding to 25 cycles of a sine wave were made;

$$A(I) = (23.0 \pm 0.2) \sin \left(\frac{\pi}{2} I \right) \quad ng$$

I = measurement number

The input acceleration is given in $ng = 0.981 \times 10^{-6} \frac{cm}{s^2}$. The experiment had to show the response of the accelerometer to this small input acceleration.

The constant acceleration (or bias) input to the accelerometer, perhaps caused by tilt, was about 17 μg. The setup is very sensitive to temperature changes; therefore, the temperature was controlled in case II (Fig. 5) and was constant to less than 0.01° C for experiment number 1 (less than 0.1° C for other runs).

Results and Discussion

The experiment had to show how to measure the small acceleration caused by mass attraction and how to define the scale factor of the accelerometer for low acceleration. Because the acceleration input was a relative change, the constant part of the data was removed from the accelerometer data AX(I) and the tilt meter data AY(I). The accelerometer data X(I) and the tilt meter Y(I) have zero mean value. These data are used for the computer analysis.

The random noise is much higher during work time than after work time. Figure 7 shows the random noise during work time. There was no
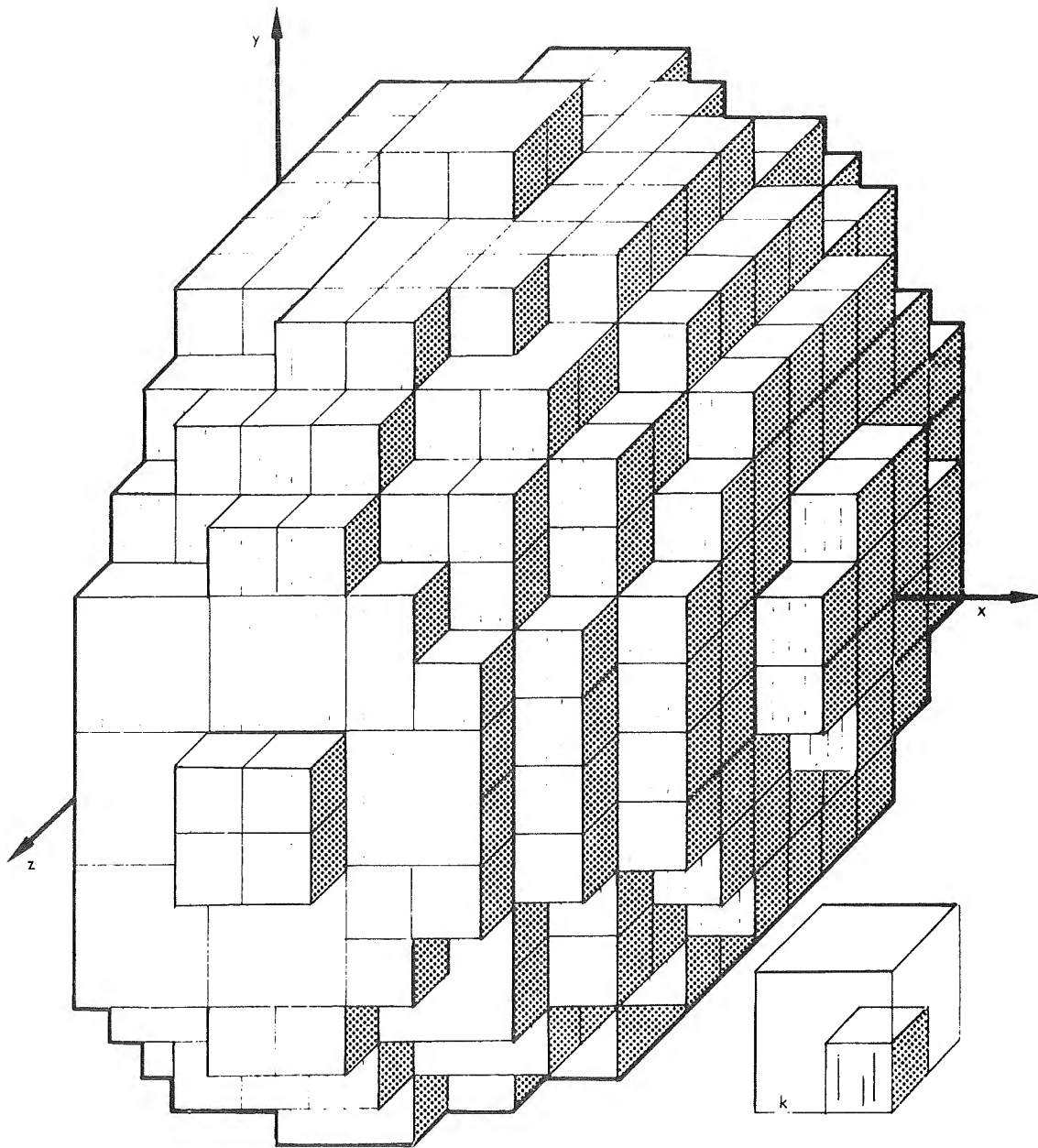
Figure 6. Attracting mass assembly.

movement of the lead mass in this experiment (run number 6). The data were collected during work time every 2 minutes with a 100-second measurement time as in the later runs with mass movement. Run number 5 is the same as run number 6 just after work time (Fig. 8). The standard deviation from an
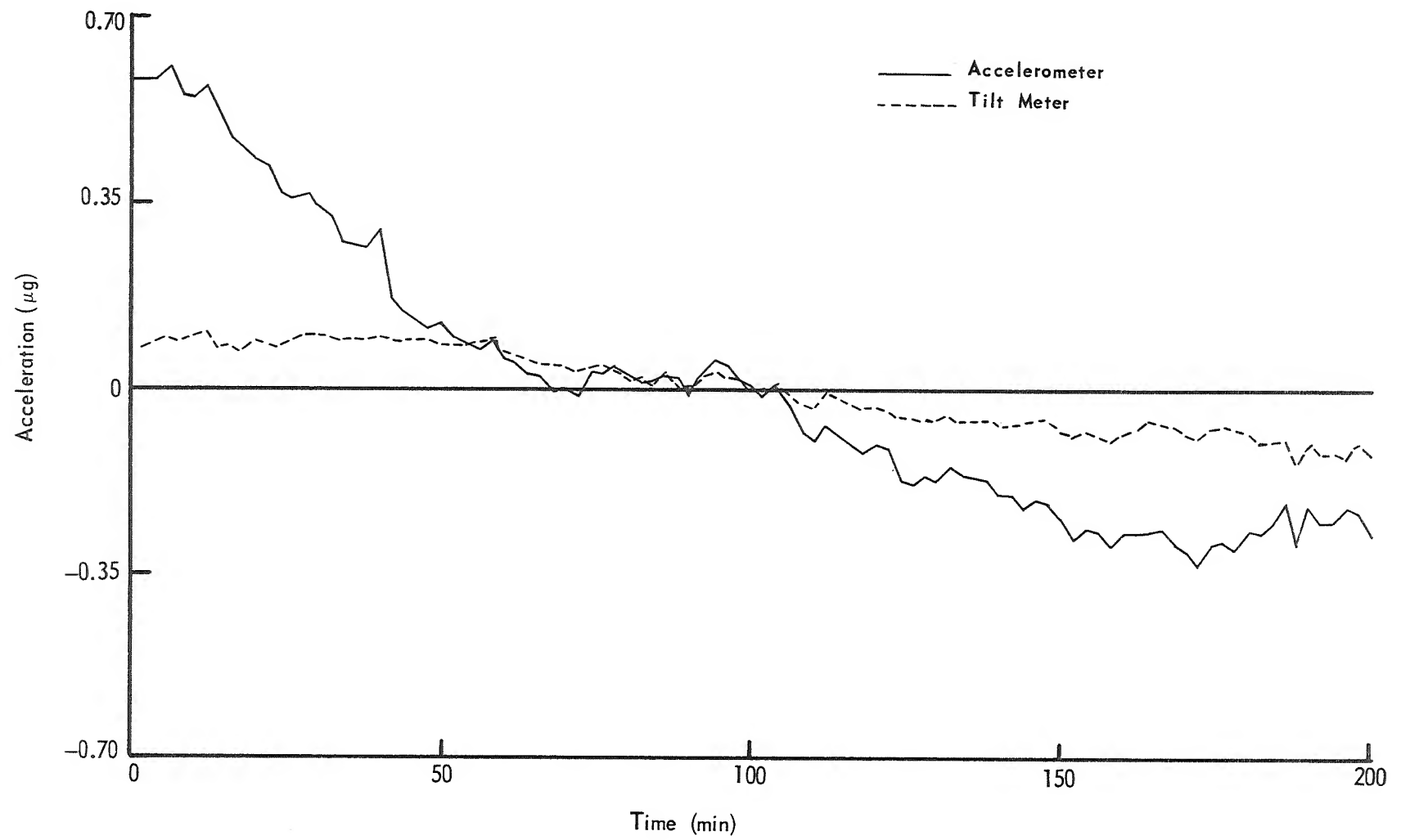
Figure 7.   Accelerometer and tilt meter data without mass attraction (during work time).
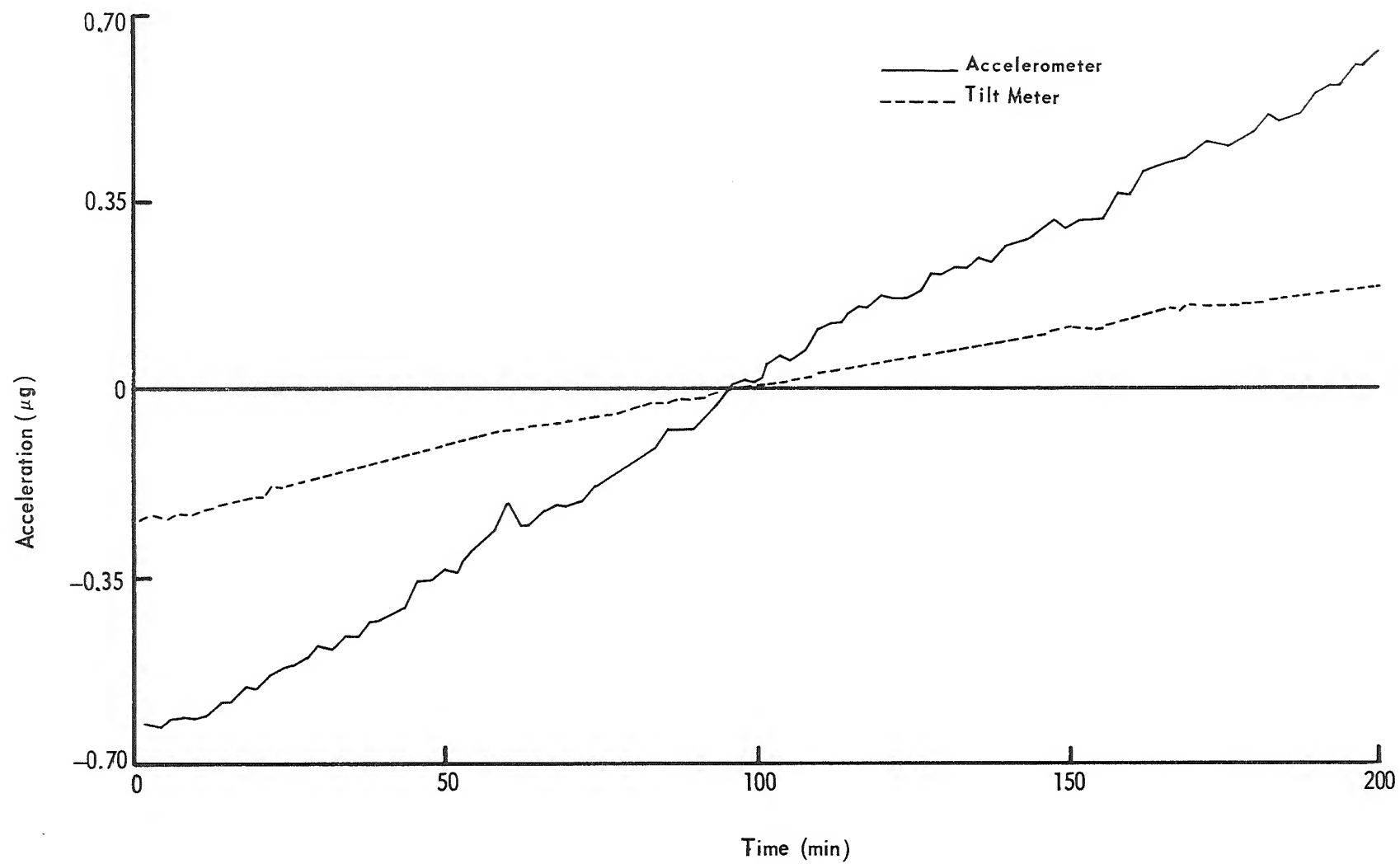
Figure 8. Accelerometer and tilt meter data without mass attraction (after work time).

adjusted curve for the run during work time is twice as much as for the run taken after work time (all the experiments were made after work time except run number 4).

The response of the accelerometer and the tilt meter to the mass attraction is overlapped by stochastic and other periodic acceleration. But already in the raw data, the movement of the mass is clear (Fig. 9). The data X(I) and Y(I) are shown in Figure 9 for run number 1 after subtracting the mean value. The time scale includes the necessary 20 seconds for moving the mass. The tilt meter data were multiplied by a scale factor to get radians that correspond to acceleration in g. The dimensions for the accelerometer data were originally impulses per second. But to give a better impression in all the graphs, the scale factor of the accelerometer data sheet is used to express the data in μg. For every experiment the first position of the lead mass was the middle position followed by the upper position.

The tilt meter data also show a very small modulation with the frequency of the mass movement. However, it is much less than the corresponding response of the accelerometer. If the accelerometer data were the result of some tilting corresponding to the mass movement, the tilt meter data would show this. The small modulation of the tilt meter data is caused by the mass attraction and is computed in Appendix C. The tilt meter is considered as a supporting device and the analysis is shown only for the accelerometer data. The accelerometer data are digital, and the analysis is made with a digital computer. A statistical analysis (autocorrelation function and power spectral density) is used together with a Fourier analysis to compute the response of the accelerometer to the small mass attraction input. The detailed analysis and data reduction techniques are given in Appendix A, and a computer program is given in Appendix B.

The acceleration input is a sine wave with a frequency of 0.0025 Hz. This input frequency corresponds for 100 measurements to a harmonic number of K=25. The unforced response evaluated for a sine wave with a frequency of 0.0025 Hz is the Fourier coefficient B(25). For a sample of 100 data X(I)

$$B(25) = 0.02 \sum_{I=1}^{100} X(I) \sin\left(\frac{2\pi}{4} \times I\right) \quad ,$$

where X(I) is the accelerometer data with zero mean value and I is the sample number. The accelerometer data X(I) in Figure 9 show the shape of a saw tooth with the frequency of 0.0025 Hz. Therefore, the Fourier analysis of the data without a data reduction has large amplitudes with low frequencies (Fig. 10). The Fourier coefficient B(25) is not just the response to the input
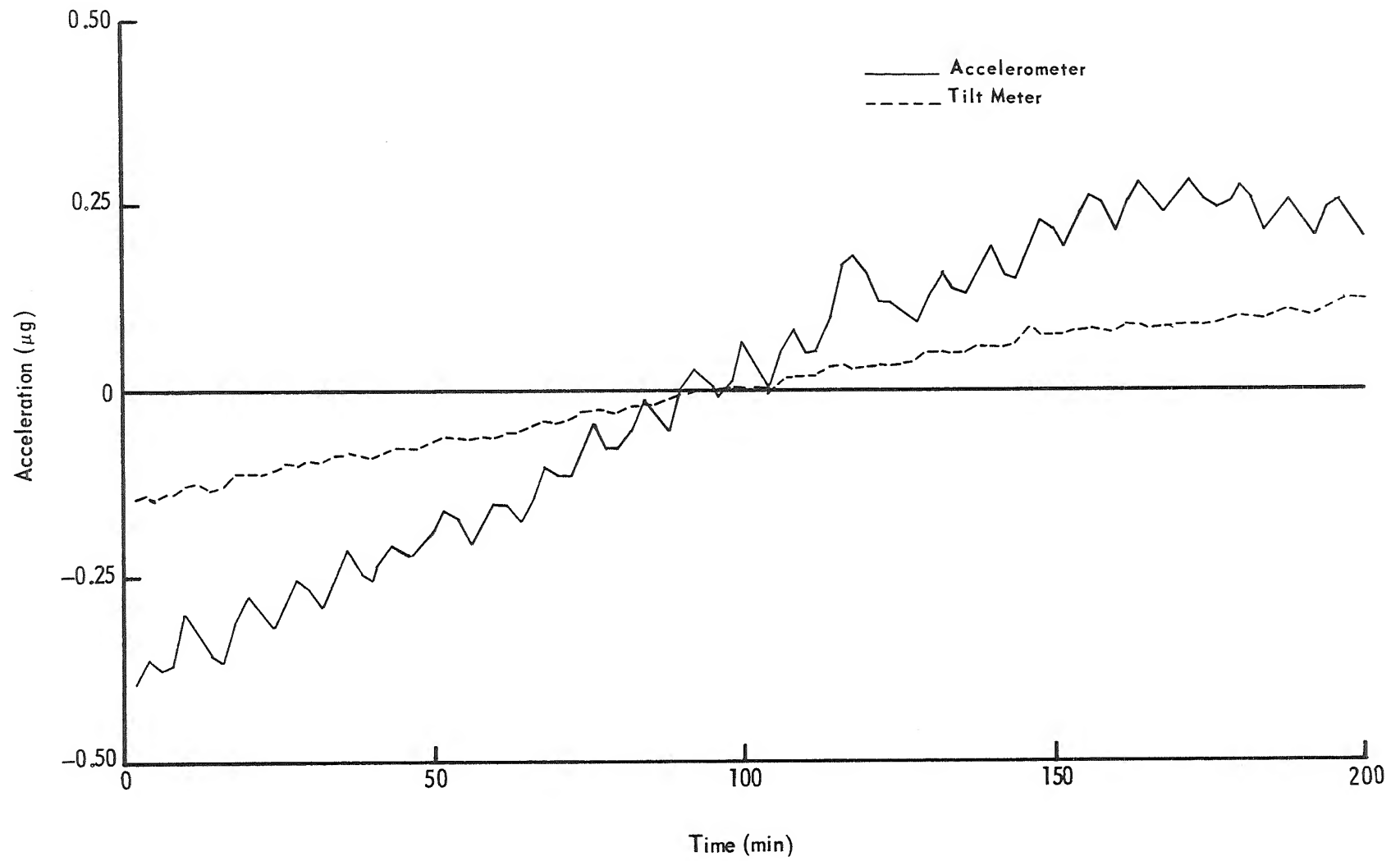
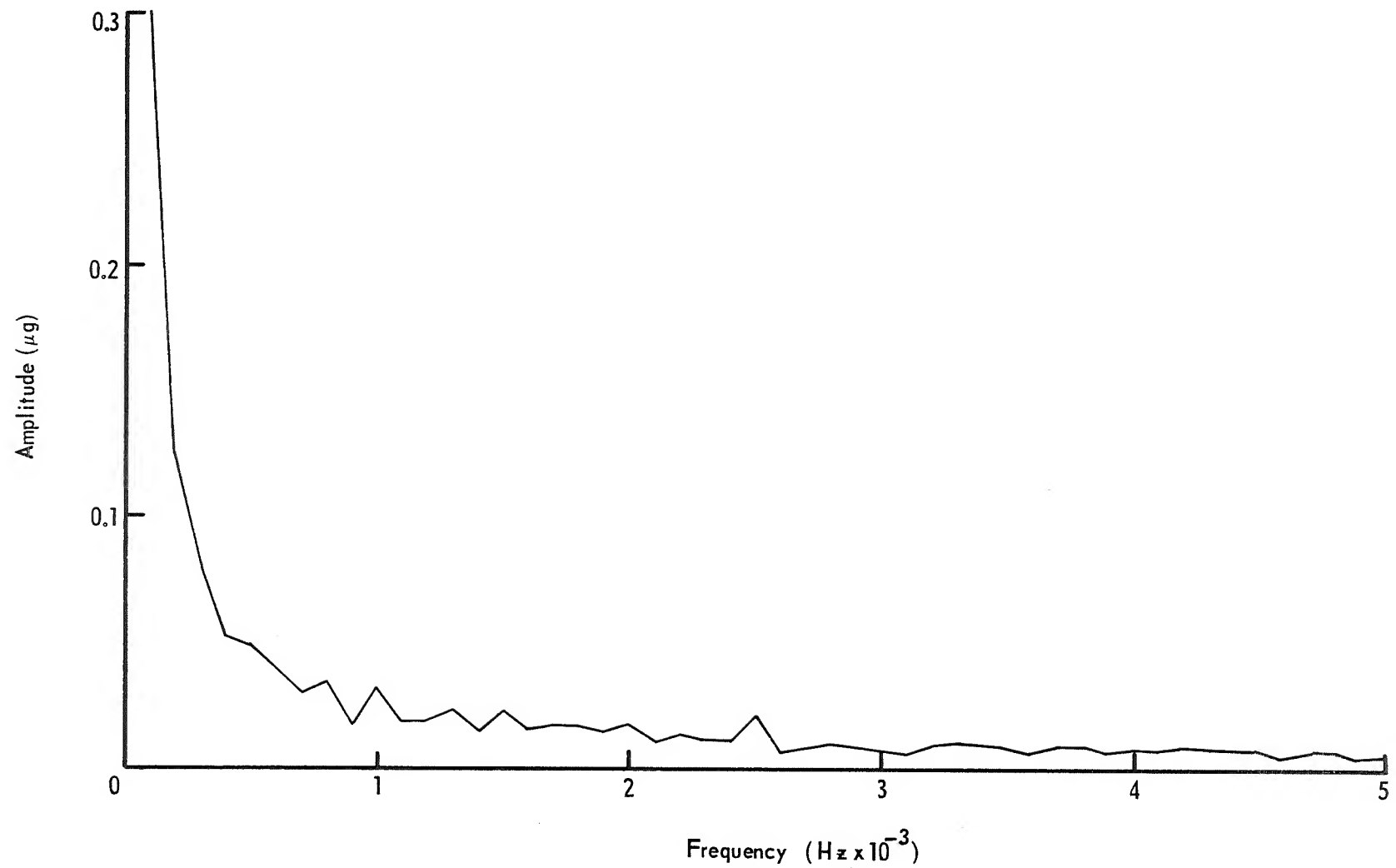Figure 9. Accelerometer and tilt meter data of experiment number 1.

Figure 10. Fourier analysis of the accelerometer data before data reduction.

17

sine wave because a certain part of the 25th harmonic is produced by the saw-toothed shape of the overall data. Therefore, several types of data reduction were tried (Appendix A); two of which were used for the calculation of the following scale factor:

1. Subtraction of XSM(I) from every X(I). XSM(I) is the mean value of the data X(I) between I−JA and I+JA. For JA=3, the summation was made over 7 points plus two edge points with a weight factor of 0.5.

2. For the error calculation, the standard deviation was computed after subtraction of the 20 highest and 20 lowest harmonics. The accelerometer data X(I) are shown in Figure 11 after the subtraction of the adjusted curve XSM(I) from X(I) with JA=3. The amplitude of the input acceleration was 23 ng at a frequency of 0.0025 Hz.

The Fourier analysis CK(K) gives the amplitude as a function of the frequency. In Figure 12, the amplitudes of two Fourier analyses are shown. The one amplitude distribution is from a run without a mass movement. This experiment is run number 5 in Table 4. The amplitude at 0.0025 Hz is almost the same as the mean value of the amplitudes at the frequencies from 0.0020 to 0.0030 Hz. The other curve in Figure 12 is the amplitude distribution of a run with a mass attraction input at a frequency of 0.0025 Hz. This run is number 1 in Table 4. The Fourier coefficient B(K) is 27.80×10^{-2} pps with a frequency of 0.0025 Hz. The mean value of the amplitudes of the harmonics from K=21 to 24 and K=26 to 29 is as low as 2.17×10^{-2} pps. The amplitude at K=25 in run number 1 is supposed to be a summation of the response to the sine-wave input and of some additional random noise. Because the bandwidth is limited, the subtraction of the mean random noise level from the amplitude at K=25 is justified. Therefore, the response of the accelerometer to the sine-wave input at 0.0025-Hz frequency is 25.63×10^{-2} pps. This value is very close to the computed one with the scale factor for higher acceleration, 23×10^{-2} pps.

The statistical analysis shows almost the same results as the Fourier analysis. The autocorrelation function RX(L) of the accelerometer data X(I) shows the periodic response to the input acceleration (Fig. 13). From the autocorrelation function, the power spectral density is computed. The amplitude G(K) of a periodic function is given by

$$G(K) = \sqrt{GX(K) \times B} \quad ,$$

where GX(K) is the power spectral density function and B is the bandwidth. The distribution of the amplitude G(K) of a smoothed power spectral density is shown as a function of the frequency in Figure 14 for run number 1. The

18
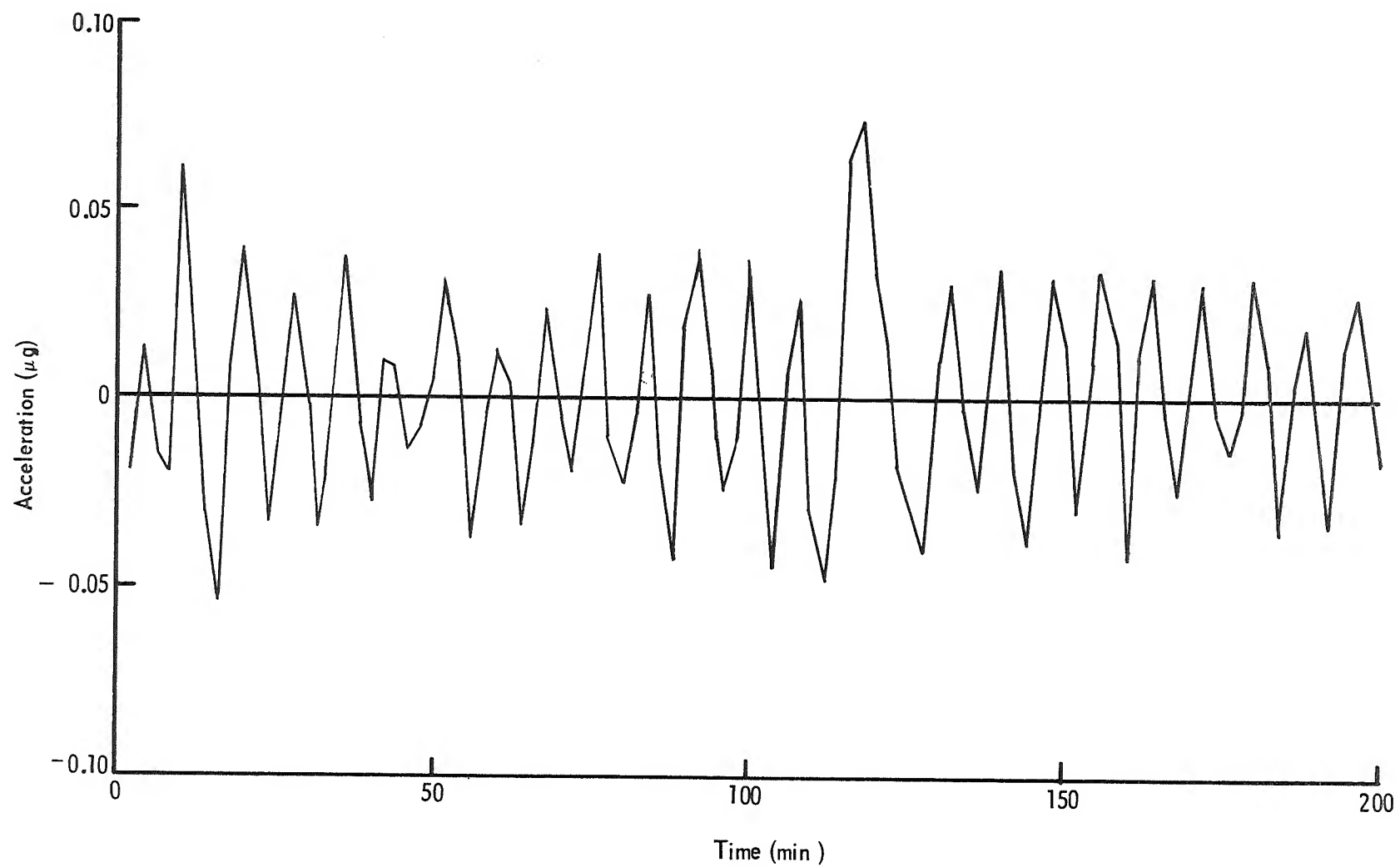
Figure 11. Accelerometer data after data reduction.

TABLE 4. RESULTS OF THE EXPERIMENTS

Experi-ment No.	NA Input Accel (ng)	Accelerometer Response		Random Noise Part		Signal Response		Standard Deviation 10^{-2} pps
		G(25) 10^{-2} pps	B(25) 10^{-2} pps	GR(25) 10^{-2} pps	CR(25) 10^{-2} pps	GO 10^{-2} pps	BO 10^{-2} pps	
1	23	28.07	27.80	4.70	2.17	23.27	25.63	5.59
2	23	26.56	26.80	3.87	3.41	22.69	23.39	6.77
3	23	29.72	29.64	5.02	5.57	24.70	24.07	11.90
Mean value for No. 1, 2, 3						24 ± 2		
4	23	24.78	25.62	5.85	5.30	18.93	20.32	14.06
5	0	2.02	1.12	2.14	2.01	−1.2	−0.89	4.90
6	0	3.14	2.08	3.94	4.13	−0.80	−2.05	10.12
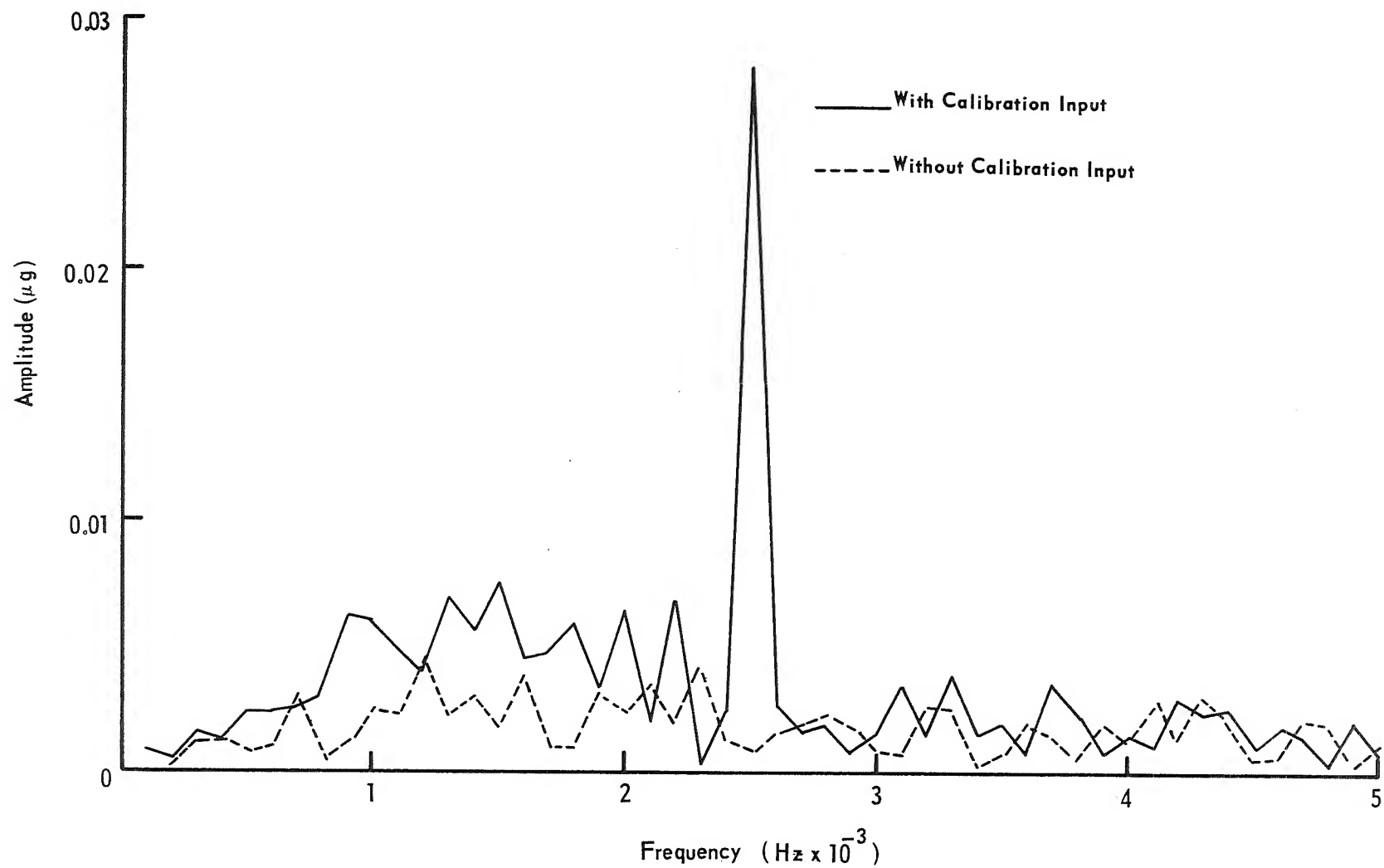
Figure 12.   Fourier analysis of the accelerometer data after data reduction.
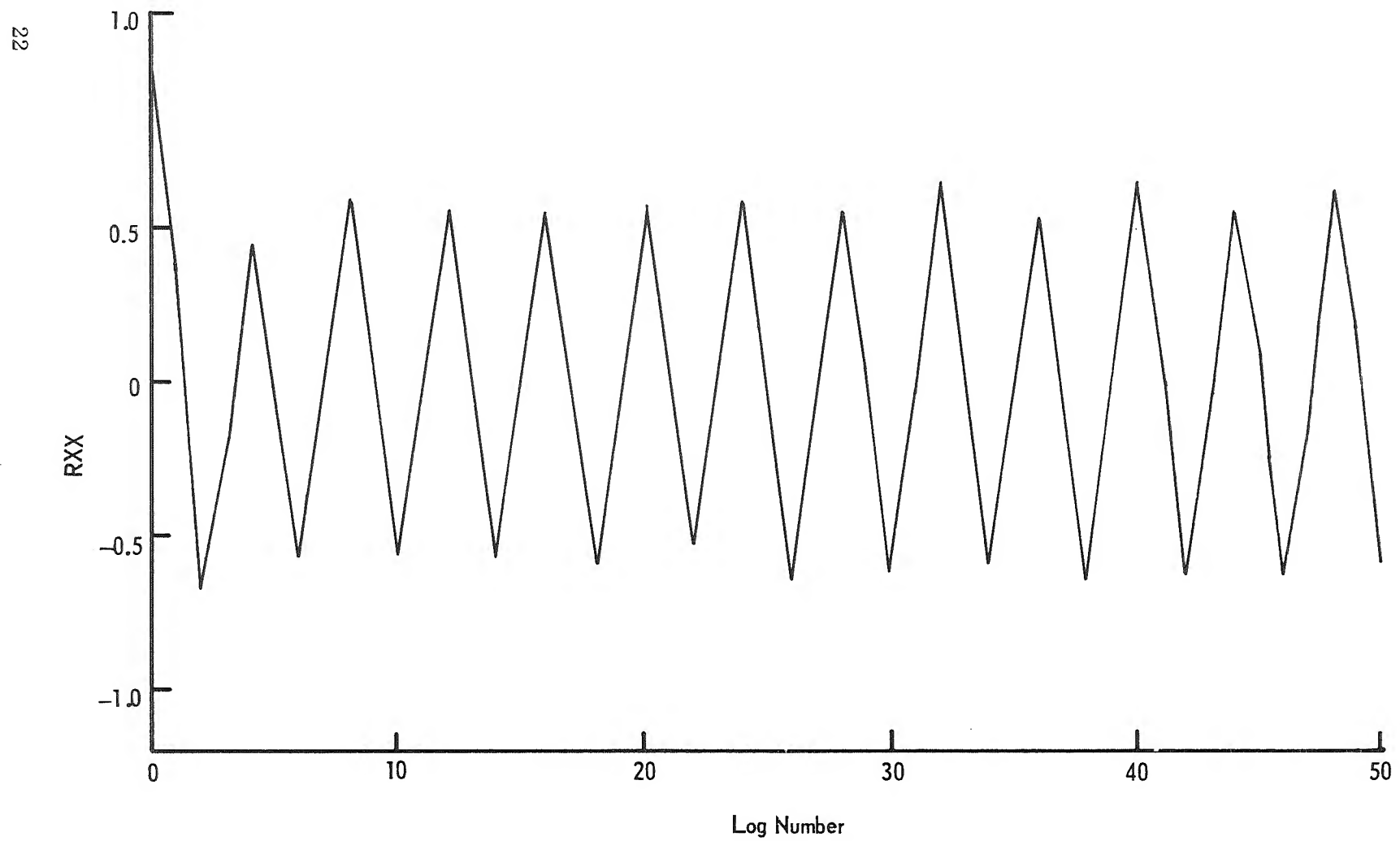
Figure 13. Autocorrelation function of the accelerometer data.
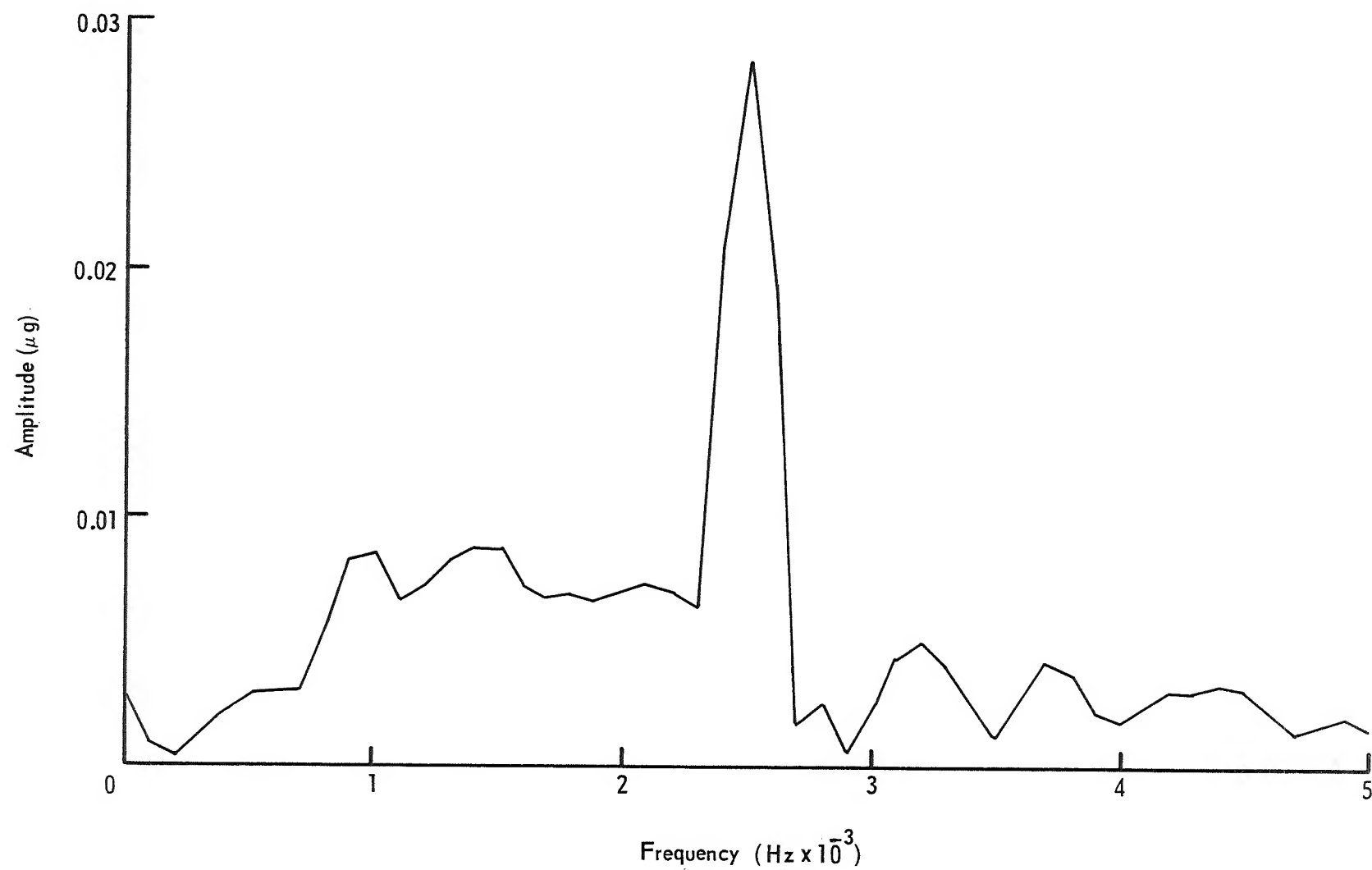
Figure 14. Smoothed power spectral density function of the accelerometer.

amplitude at the frequency 0.0025 Hz is $G(25)=28.07\times10^{-2}$pps. The mean value of the random noise for the frequency FO is $GR(25)=4.70\times10^{-2}$pps and the response to the sine wave at the frequency of 0.0025 Hz is therefore 23.27×10^{-2}pps.

For the error calculation, the 20 higher and 20 lower harmonics of the Fourier analysis are subtracted. This does not change the amplitude of the 25th harmonic. After this filtering, the standard deviation from the ideal response sine wave with the amplitude B(25) is calculated. This is $XSD = 5.59\times10^{-2}$pps for run number 1, which was made after work time with a very low noise level. Runs 2 and 3 were made under almost the same conditions, except that the noise level was higher because of the air-conditioning equipment. Run number 4 was made during working hours; because of the high noise level, the data could not be used for scale factor calculations.

The mean value of the response to the mass attraction input is for the first three numbers,

$$AM = (24 \pm 2) \times 10^{-2}\text{pps} .$$

This gives a scale factor $SC=(1.04\pm0.09)\times10^{7}$pps/g for the input amplitude of 23.0 ng. This result is very close to the scale factor of the data sheet in the higher acceleration with 1.02×10^{7}pps/g.

The size of the error for the scale factor could be reduced by an improved setup incorporating better noise isolation and automatic and larger movement of the attracting lead mass. For larger movement of the mass, the amplitude of the input sine wave could be twice as high, and the calibration would be more accurate. The experimental setup was more or less improvised. The aim of the experiments was to prove that the calibration with a mass attraction in the low g range of 10^{-8} g is possible with good confidence and repeatability. The application of these experiments to the calibration of an accelerometer in a satellite for the measurement of the gravity gradient anomalies of the moon is proposed.

CALIBRATION IN ORBIT

The accelerometer gets a large acceleration during the boosting phase of the rocket. Therefore, the state of the art of the accelerometer requires

a switching to the highly sensitive mode after the start of free flight. After this point, there are no large accelerations and the mass center of the satellite is almost under 0-g conditions. The threshold of the accelerometer can be set very low, but there is no way to calibrate the accelerometer in this high sensitive range with the generally used terrestrial means. There are many different unknown acceleration inputs to the accelerometer in a satellite; that is, gravity gradient acceleration of the orbited planet, mass attraction by the satellite, low thrust impulses, etc. This paper proposes the calibration of the accelerometer in the satellite by using a well known but variable mass attraction scheme. A reasonable size of the mass for the calibration in a satellite might be 4 kg, which sets the upper limit of the acceleration to 10^{-9} g (Table 1). The required threshold of an accelerometer in the lunar gravity gradient anomalies measurement is lower than 10^{-10} g. The acceleration input caused by mass attraction can be varied by changing the distance or the component of mass attraction along the accelerometer input axis. The changing of the component has some advantages. The accelerometer is fixed in relation to the satellite. The mass can be turned around the accelerometer continuously with a small angular velocity. The input acceleration is a cosine function for the arrangement in Figure 15. The argument of the cosine is the angle between the input axis and the line from the center of the proof mass to the center of the calibrating mass. For easy data handling, the rotation axis of the calibrating mass should go through the center of the accelerometer proof mass. If there is no other time variable input, the response of the accelerometer is a cosine function with an additional constant caused by the constant mass attraction input of the satellite. With a small computation, the scale factor, nonlinearity, and constant bias of the accelerometer can be calculated. The
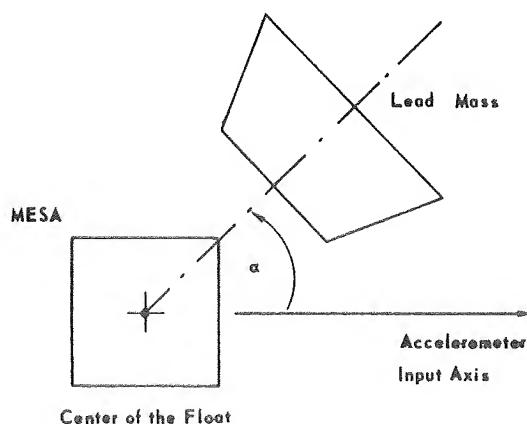
Figure 15. Calibration of a single-axis accelerometer in a satellite by mass attraction.

movement of the mass around the accelerometer can be a continuous one or in steps to facilitate digital analysis. The calibration does not interfere with the experiment and can continue through the whole measurement.

CONCLUSIONS

The calibration of an accelerometer in the laboratory by the mass attraction method may be of interest in the future, when the low accelerometer thresholds are required. In orbit, the mass attraction scheme is the only presently known practical calibration scheme for accelerations below 10^{-9} g.

APPENDIX A

DATA HANDLING FOR THE LABORATORY CALIBRATION OF AN ACCELEROMETER USING THE MASS ATTRACTION PRINCIPLE

The measurements of every experiment are numbered from I=1 to N. The input acceleration A was a sine wave with KO=4 positions per wave length (cycle)

$$A(I) = NA \sin \frac{2\pi}{KO} \quad (I-1)$$

$$I = 1, 2, \ldots, N$$

$$NA = 23.0 \times 10^{-9} \text{ g}$$

$$N = 100 = \text{number of measurements}$$

$$KO = 4 = \text{number of measurements per cycle.}$$

There are two equal sets of N data; the MESA data, AX(I) (an integer number of impulses per H = 100-second measurement time) and the tilt meter data AY(I) (an integer number from the integrating digital volt meter). The mean values of the original data are

$$XM = \frac{1}{N} \sum_{I=1}^{N} AX(I)$$

$$YM = \frac{1}{N} \sum_{I=1}^{N} AY(I)$$

for $I = 1, 2, \ldots, N$.

26

The data are transformed to data with zero mean value

$$X(I) = AX(I) - XM$$

$$Y(I) = AY(I) - YM$$

These data, $X(I)$ and $Y(I)$, are used for the analysis of the MESA data, $AX(I)$.

Data Analysis

The highest frequency in the data should be lower than the Nyquist frequency (FN), which is half the sampling rate. Thus $FN = \dfrac{1}{2H}$ and H = sampling time. The sampling time H was for every measurement 100 seconds, giving a Nyquist frequency of $FN = 0.005$ Hz. The input frequency of the mass movement is $FO = 0.0025$ Hz.

The statistical analysis uses the autocorrelation function and the power spectral density function. The autocorrelation function of $X(I)$ is given by

$$RX(L) = \frac{1}{N-L} \sum_{I=1}^{N-L} X(I) \times X(I+L) \quad ,$$

when L = lag number 1 to $N/2$ and N = number of samples = 100. The normalized autocorrelation function $RXO(L)$ is obtained by dividing $RX(L)$ by $RX(0)$.

The cross-correlation function of the MESA data, $X(I)$, with the tilt meter data, $Y(I)$, is

$$RXY(L) = \frac{1}{N-L} \sum_{I=1}^{N-L} X(I) \times Y(I+L)$$

$$\text{for } L = 1, 2, \ldots, \frac{N}{2} \quad .$$

A raw estimate of the power spectral density is [8,9],

$$GX(K) = 2H \times \left[RX(0) + 2 \times \sum_{L+1}^{ML-1} RX(L) \times \cos\left(\frac{\pi LK}{ML}\right) + (-1)^K \times RX(ML) \right],$$

where

K = harmonic number

H = sampling interval

ML = maximum lag number

L = lag number.

The frequency for the PSD is

$$F(K) = \frac{K}{2 \times ML \times H} \quad ,$$

and the bandwidth is

$$B = \frac{1}{ML \times H} \quad .$$

GX(K) is given in units $^2/B$.

The amplitude versus frequency is, for a periodic function,

$$G(K) \approx \sqrt{GX(K) \times B} \quad .$$

For the analysis, the nonsmoothed PSD is used.

The Fourier analysis is also used to calculate the amplitude of periodic functions. The Fourier coefficients for the MESA data, X(I), are

$$A(K) = \frac{2}{N} \sum_{I=1}^{N} X(I) \cos\left(\frac{2\pi K}{N} I\right) \qquad K = 1, 2, \ldots, \frac{N}{2}$$

$$B(K) = \frac{2}{N} \sum_{I=1}^{N} X(I) \sin\left(\frac{2\pi K}{N} I\right) \qquad K = 1, 2, \ldots, \frac{N}{2}$$

$$A(0) = 0 \quad ,$$

where

N = number of data (even)

K = harmonic number.

The frequency of the Fourier components is

$$F(K) = \frac{K}{N \times H} = K \times 10^{-4} \text{ Hz}$$

Because the maximum lag number in the statistical analysis was chosen to be $ML = \frac{N}{2}$, the frequency of the Fourier analysis agrees with the frequency of the PSD for the same K.

Data Reduction

The amplitudes of the lower harmonics in the data analysis are larger than the observed amplitude at the frequency FO of the acceleration input. To unmask the amplitude at frequency FO, four types of data reduction are available in the computer program (Appendix B). First, the trace of the tilt meter is subtracted from the MESA data after the adjustment by a factor P. The factor P is calculated with the least mean square fit method [10]

$$\sum_{I=1}^{N} \left[X(I) - P \times Y(I) \right]^2 = \text{Min}$$

$$P = \frac{\Sigma \; X(I) \times Y(I)}{\Sigma \; Y(I) \times Y(I)} \qquad .$$

The reduced data are

$$XR(I) = X(I) - P \times Y(I)$$

for $I = 1, 2, \ldots, N.$

The second type of reduction is a filtering by subtraction of the lower and higher harmonics

$$XR(I) = X(I) - \sum_{K=1}^{10} \left[A(K) \cos \frac{2\pi KI}{N} + B(K) \sin \frac{2\pi KI}{N} \right]$$

$$- \sum_{K=40}^{50} \left[A(K) \cos \frac{2\pi KI}{N} + B(K) \sin \frac{2\pi KI}{N} \right] \qquad .$$

$A(K)$ and $B(K)$ are the Fourier coefficients computed in the previous data analysis.

The third reduction is the most effective one to filter out the sine wave with the wavelength $KO \times H$. From every data point $X(I)$, a mean value of the S closest points is subtracted to get the reduced data $XR(I)$.

$$XR(I) = X(I) - \frac{1}{2S} \left\{ \left[0.5 \times X(I-S) + \sum_{J=I-S+1}^{I+S-1} \right] \left[X(J) + 0.5 \times X(I+S) \right] \right\};$$

2S must be a multiple of the sample number KO per wavelength to avoid changing the amplitude at the frequency FO.

In several experiments, the data $X(I)$ build almost a straight line that is modulated by a sine wave with the frequency FO. Therefore, the subtraction of the adjusted straight line would reduce the data, but it is not

sufficient in every case. After reduction the data again go through the analysis. The standard deviation XSD of the reduced and filtered data XR(I) from the idle or unforced response to the sine wave contains the random noise and is considered as a good approximation of the error,

$$XSD = \left\{ \frac{1}{N} \ \Sigma \left[XR(I) - B(25) \ \sin \left(\frac{2\pi}{4} \ I \right) \right]^2 \right\}^{1/2}$$

RX(I) = reduced and filtered data

B(25) = Fourier coefficient of the 25th harmonic.

The XSD with the amplitude G(25) of the power spectral density gives the same value as with the Fourier coefficient B(25).

APPENDIX B

COMPUTER PROGRAM FOR
DATA ANALYSIS AND REDUCTION

This program is written in FORTRAN II for the GE235 digital computer. The arrangement of the program and the data follows.

1. SLEM (computer control cards)

2. Main program

3. Subroutine plot

4. Data card   1/2

5. For data input   0   Format (I4)

    For program test 1   Format (I4)

6. Experiment card N, NH, ML, NA, MN, MAXL,
    MAXK, KO, MON, MD   Format (10(I4))

7. MESA data AX(I)   Format (5(3XI6, 1X))

8. Tilt meter data AY(I)   Format (5(2XI8, 1X))

9. Sample number with   KM(I)   Format (I4)
    wrong data

10. Data reduction IC   Format (I4)
              MA or JA   Format (I4)

11. End   -1   Format (I4)

The subroutine plot is for plotting the data on the initial printout.

```
C       CALIBRATION OF THE MESA

        KOMMON           Y[100],XSM[100],RYY[50],Q[50],
       1RX[51],RY[51],RXY[51],RYX[51],GY[51],
       2RXYO[50],AX[600],KM[20],AY[600],GXO[50],F[50],
       3KL[600],GXX[50],AK[50],BK[50]
        DIMENSION X[100],RXX[100],GX[100],CK[100],GXA[100]
        PI=3.141592654
        PI2=6.283185308
     13 READ 201,KT
    201 FORMAT [I4]
        IF [KT] 217,210,202


C       TEST OF THE PROGRAM

    202 READ 203,N,NH,MAXL,MAXK,LXS,KXS,LXC,KXC,LY,KY,KO
    203 FORMAT [4[I4],3[I8,I4],I4]
        KM[1]=N+2
        ML=N+5
        NA=100
        MN=1
        ZLXS=LXS
        ZKXS=KXS
        ZLXC=LXC
        ZKXC=KXC
        ZLY=LY
        ZKY=KY
        PRINT 6,LXS,KXS,LXC,KXC
      6 FORMAT[21H1          TEST   X[I] = I8,15H  SIN[2*PI*ZL/ I4,
       16H ]   + I8,15H  COS[2*PI*ZL/ I4,3H ] ]
        PRINT 18,LY,KY
     18 FORMAT[22H                 Y[I] = I8,
       115H  COS[2*PI*ZL/ I4,3H ] ]
        DO 204 L=1,ML
        ZL=L-1
        KL[L]=ZLXS*SINF[PI*ZL/ZKXS]+ZLXC*COSF[PI*ZL/ZKXC]
    204 AX[L]=KL[L]
        DO 205 L=1,ML
        ZL=L-1
        KL[L]=ZLY*COSF[PI*ZL/ZKY]
    205 AY[L]=KL[L]
        GO TO 206


C       READING AND ARRANGING OF THE DATA

    210 READ 1,N,NH,ML,NA,MN,MAXL,MAXK,KO,MON,MD
      1 FORMAT [10[I4]]
        READ 102,[KL[L],L=1,ML ]
    102 FORMAT [5[ 3XI6,1X]]
        DO 71 L=1,ML
     71 AX[L]=KL[L]
        READ 103,[KL[L],L=1,ML]
    103 FORMAT [5[ 2XI8,1X]]
        DO 73 L=1,ML
     73 AY[L]=KL[L]
```

```
C       CALIBRATION OF THE MESA

                READ 201,(KM[I],I=1,MN)
        206 ZN=N
                H=NH
                ZKO=KO
                ZML=ML
                ZNA=NA
                ZMN=MN
                IC=1
                PRINT 26
        26 FORMAT [1H1]
                PRINT 106,[AX[L],L=1,ML]
        106 FORMAT [5[F12,1]]
                PRINT 106,[AY[L],L=1,ML]
                PRINT 201,[KM[L],L=1,MN]

                DO 11 I=1,MN
                K=KM[I]
                M=ML-I
                DO 11 L=K,M
                AX[L]=AX[L+1]
        11 AY[L]=AY[L+1]

                M=MAXL
                ZM=M
                ZMAXK=MAXK
                ZMAXL=MAXL
                A=0
                B=0
                DO 17 I=1,N
                X[I]=AX[I]
                A=A+AX[I]
        17 B=B+AY[I]
                XM=A/ZN
                YM=B/ZN
                DO4 I=1,N
                AX[I]=AX[I]-XM
        4 Y[I]=AY[I]-YM
                ID=0
        216 READ 201,IC
                GO TO [ 16,119,129,139,149,13],IC


C       DATA ANALYSIS
C       ************

        16 ID=ID+1
                IB=100*ID+IC
                A=0
                B=0
                DO 20 I=1,N
                X[I]=X [I]-XM
                A=A+X[I]*X[I]
        20 B=B+Y[I]*Y[I]
                RXO=A/ZN
                RYO=B/ZN
```

34

```
C       CALIBRATION OF THE MESA

        XSD=SQRTF(ABSF(RXO))
        YSD=SQRTF(ABSF(RYO))
        PRINT 8,IB,MON,MD
      8 FORMAT (45H1 CALIBRATION OF THE MESA                    I4,
       15XI4,1H/I2//)
        PRINT 74,(X(I),Y(I),I=1,N)
     74 FORMAT (2(E12.4))
        CALL PLOT(X,N)


C       AUTOCORRELATION OF X(I)

        DO 24 L=1,M
        A=0
        K=N-L
        ZK=K
        DO 21 I=1,K
        IL=I+L
     21 A=A+X(I)*X(IL)
     22 RX(L)=A/ZK
     24 RXX(L)=RX(L)/RXO


C       AUTOCORRELATION OF Y(I)

        DO 34 L=1,M
        K=N-L
        ZK=K
        A=0
        DO 31 I=1,K
        IL=I+L
     31 A=A+Y(I)*Y(IL)
     32 RY(L)=A/ZK
     34 RYY(L)=RY(L)/RYO
        B=RXO**.5
        C=RYO**.5
        D=B*C


C       CROSSCORRELATION OF X(I) AND Y(I)

        DO 44 L=1,M
        Q(L)=L
        K=N-L
        A=0
        ZK=K
        DO 41 I=1,K
        IL=I+L
     41 A=A+X(I)*Y(IL)
        RXY(L)=A/ZK
     44 RXYO(L)=RXY(L)/D
        PRINT 8,IB,MON,MD
        PRINT 81
     81 FORMAT (80H  L       RX        RY        RXY       RXX
       1 RXY      RXYO        //)
```

```
C        CALIBRATION OF THE MESA                    .
           RC=0
           DO 33 I=1,N
        33 RC=RC+X[I]*Y[I]
           RCO=RC/D
           A=0
           B=1.0
           PRINT 30,A,RXO,RYO,RC,A,B,RCO
        30 FORMAT [F6.1,3[E12.4], 2X3[F10.5]]
           DO 84 L=1,M
        84 PRINT 30,   Q[L],RX[L],RY[L],RXY[L],RXX[L],RYY[L],RXYO[L]
           PRINT 112
       112 FORMAT [ /]
           PRINT 2,XM,YM
         2 FORMAT[6H XM = E12.4, 6H YM = E12.4 ]
           PRINT 12,XSD,YSD
        12 FORMAT[6H XSD= E12.4, 6H YSD= E12.4///]
           CALL PLOT[RXX,M]


C        POWERSPECTRUM OF X[I]

           PRINT 8,IB,MON,MD
           PRINT 91
        91 FORMAT[64H    K      FREQUENCY    RAW PSD      AMPLIT .  SMOOTH PSD
         1   AMPLIT //]
           M=MAXK
           MK = M-1
           ZM=M
           BF=1.0/[ZM*H]
           DO 54K=1,M
           Q[K]=K
           ZK=K
           F[K]=0.5*ZK/[ZM*H]
           A=0
           B=0
           DO 53 L=1,MK
           ZL=L
        53 A=A+RX[L]*COSF[PI*ZL*ZK/ZM]
           GX[K]=2.0*H*[RXO+2.0*A+RX[M]*[-1.0]**K]
        54 GXA[K]=[BF*ABSF[GX[K]]]**0.5
           AB=0
           BX=0
           DO 109 L=1,MK
       109 AB=AB+RX[L]
           BX=0.5*[AB +     GX[1]]
           AB=2.0*H*[RXO+2.0*AB+RX[M]]
           AXO=[ABSF[BX*BF*2.0]]**0.5
           A=0
           S=SQRTF[ABSF[AB*BF]]
           PRINT 19,A,A,AB,S,BX,AXO
        19 FORMAT [F6.1,5[E12.4]]
           GXX[1]= 0.5*GX[1]+0.25*[AB+GX[2]]
           DO 311 K=2,MK
           KR=K-1
           KP=K+1
```

```
C      CALIBRATION OF THE MESA

   311 GXX[K] = 0.25*GX[KP]+0.5*GX[K]+0.25*GX[KF]
       GXX[M]=0.5*GX[MK]+0.5*GX[M]
       DO 312 K=1,M
   312 GXO[K]=[ABSF[GXX[K]]*BF*2.0]**0.5
       DO 93 K=1,M
    93 PRINT 19, Q[K],F[K],GX[K],GXA[K],GXX[K],GXO[K]
       PRINT 112
       PRINT 3,BF
     3 FORMAT [13H   BANDWIDTH = E12.4, 5H   HZ //]
       CALL PLOT[GXA,M]


C      FOURIER ANALYSIS

       DO 403 K=1,50
       ZK=K
       F[K]=ZK/[H*ZN]
       A=0
       B=0
       DO 402 I=1,N
       ZI=I-1
       A=A+X[I]*COSF[PI2*ZI*ZK/ZN]
   402 B=B+X[I]*SINF[PI2*ZI*ZK/ZN]
       AK[K]=2.0*A/ZN
       BK[K]=2.0*B/ZN
   403 CK[K]=[AK[K]**2.0+BK[K]** 2.0]**0.5
       PRINT 8,IB,MON,MD
       PRINT 404
   404 FORMAT[52H   K     FREQUENCY        AK          BK          CK
       DO 405 K=1,50
   405 PRINT 406,Q [K],F[K],AK[K],BK[K],CK[K]
   406 FORMAT[F6,1,4[E12,4]]
       PRINT 112
       PRINT23
    23 FORMAT [ 85H       N            H          ML       INPUT ACC
      1NR OF ERRORS     MAX L      MAX K]
       PRINT 105,ZN, H,ZML,ZNA,ZMN,ZMAXL,ZMAXK
   105 FORMAT [7[F12,1]]
       CALL PLOT[CK,50]


C      STANDARD DEVIATION OF X[I] TO XINP

       A=0
       XINP=ZNA*10.0**[-9.0]
       SK1=BK[25]/XINP
       DO 127 I=1,N
       ZI=I-1
       U    =X[I]-BK[25]*SINF[1.570796327*ZI]
   127 A=A+U*U
       SD1=SQRTF[A/ZN]
       ESK1=SD1*SK1/BK[25]
       MS=M/2
       SK2=GXA[MS]/XINP
       A=0
```

```
C       CALIBRATION OF THE MESA

            DO128 I=1,N
            ZI=I-1
            U   =X(I)-GXA(MS)*SINF(1.570796327*ZI)
128   A=A+U*U
            SD2=SQRTF(A/ZN)
            ESK2=SD2*SK2/GXA(MS)
            PRINT 8,IB,MON,MD
            PRINT 121,XINP
121   FORMAT(25H INPUT ACCELERATION  A = E12.4,
            122H SIN(2*PI*(I-1)/ 4)   G //)
            PRINT 122,BK(25),SD1
122   FORMAT(25H OUTPUT (FOURIER)    B =(E12.4,3H + F12.4,
            128H)SIN(I*PI*(I-1)/ 4)  IMP/SEC //)
            PRINT 123,GXA(MS),SD2
123   FORMAT(25H OUTPUT (PSD)        C =(E12.4,3H + E12.4,
            128H)SIN(I*PI*(I-1)/ 4)  IMP/SEC //)
            PRINT 124
124   FORMAT(34H SCALEFACTOR FOR VERY LOW G-INPUT //)
            PRINT 125,SK1,ESK1
125   FORMAT(21H             SC(FOUR) = E12.4,3H + F12.4,
            114H  IMP/SEC/G   //)
            PRINT 126,SK2,ESK2
126   FORMAT(21H             SC(PSD)  = E12.4,3H + F12.4,
            114H  IMP/SEC/G   //)
            GO TO 216


C       DATA REDUCTION
C       ****************


C       LEAST MEAN-SQUARE FIT  WITH TILT DATA

119 A=0
            B=0
            DO 9 I=1,N
            B=B+AY(I)*AY(I)
9   A=A+AX(I)*AY(I)
            A=A/B
            B=0
            DO 10 I=1,N
            X(I)=AX(I)-A*AY(I)
10  B=B+X(I)
            XM=B/ZN
            GOTO 16


C       SUBTACTION OF A STRAIGHT LINE

129 A=0
            DO 400 I=1,9
400 A=A+AX(I)
            XA1=A/9,0
            NL=N-8
            A=0
```

PROGRAM LISTING (Continued)

```
C      CALIBRATION OF THE MESA

       DO 401 I=NL,N
401    A=A+AX[I]
       XA2=A/9.0
       A=0
       DO 413 I=1,N
       ZI=I
       X [I]=AX[I]-XA1-[XA2-XA1]*[ZI-5.0]/91.0
413    A=A+X[I]
       XM=A/ZN
       GO TO 16


C      SUBTRACTION OF THE LOWER AND HIGHER HARMONICS

139    A=0
       READ 201,MA
       MB=50-MA
       DO410 I=1,N
       ZI=I-1
       B=0
       DO 411 K=1,MA
       ZK=K
411    B=B+AK[K]*COSF[PI2*ZI*ZK/ZN]+BK[K]*SINF[PI2*ZI*ZK/ZN]
       DO 412 K=MB,50
       ZK=K
412    B=B+AK[K]*COSF[PI2*ZI*ZK/ZN]+BK[K]*SINF[PI2*ZI*ZK/ZN]
       X[I]= X[I]-B
410    A=A+X[I]
       XM=A/ZN
       GOTO 16


C      SUBTRACTION OF AN ADJUSTED CURVE

149    READ 201,JA
       ZJA=[JA+1]*2
       JB=JA+2
       JC=100-JA-1
       JD=100-JA
       DO 701 I=JB,JC
       MA=I-JA
       MB=I+JA
       MA1=MA-1
       MB1=MB+1
       A=0
       DO 700K=MA,MB
700    A=A+AX[K]
701    XSM[I]=[A+0.5*[AX[MA1]+   AX[MB1]]]/ZJA
       JA1=JA+1
       DO 703 I=3,JA1
       LK=2*[I-1]
       ZLK=LK
       LK1=LK+1
       A=0
       DO 702 K=2,LK
```

39

```
C     CALIBRATION OF THE MESA
      702 A=A+AX[K]
      703 XSM[I]=[A+0.5*[AX[1]+      AX[LK1]]]/ZLK
          XSM[1]=.5*[AX[1]+   AX[2]]
          XSM[2]=[.5*AX[1]*AX[2]+.5*AX[3]]*.5
          DO 705 I=JD,98
          LK=2*I-99
          ZLK=2*[100-I]
          LK1=LK-1
          A=0
          DO 704 K=LK,99
      704 A=A+AX[K]
      705 XSM[I]=[A+.5*[AX[100]+     AX[LK1]]]/ZLK
          XSM[99]=.5*[AX[99]+.5*[AX[98]*AX[100]]]
          XSM[100]=.5*[AX[99]+    AX[100]]
          A=0
          DO 706 I=1,N
          X[I]=AX[I]-XSM[I]
      706 A=A+X[I]
          XM=A/ZN
          GO TO 16
      217 STOP
          END
```

```
      SUBROUTINE PLOT (Y,N)
      DIMENSION Y(100),K(120),YMIN(11)
      YMIN(1)=Y(1)
      YMAX =Y(1)
      DO 1 I=1,N
      YMIN(1)=MIN1F(YMIN(1),Y(I))
1     YMAX=MAX1F(YMAX,Y(I))
      DO 2 I=2,11
2     YMIN(I)=(YMAX-YMIN(1))/10.+YMIN(I-1)
      PRINT 3
3     FORMAT (1H1///)
      PRINT4,(YMIN(I),I=1,11)
4     FORMAT (7X11(1XE9.2))
      PRINT5
5     FORMAT (14X101H(---------I---------I---------I---------I--------
     1--------I---------I--------I---------I---------I)
      X=1.0
      DO9I=1,N
      DO6IJ=10,120
6     K(IJ)=199728
      DO7L=15,115,10
7     K(L)=105520
      NN=((Y(I)-YMIN(1))/(YMAX-YMIN(1)))*100.+15.5
      K(NN)=133344
      PRINT8,X,(K(M),M=10,120)
8     FORMAT(1H F7.1,1X,6A1,15A1,15A1,15A1,15A1,15A1,15A1,15A1)
9     X=X+1.0
      RETURN
      END
```

APPENDIX C

MASS ATTRACTION OF THE TILT METER

The level in the mercury pools of the tilt meter changed with the positions of the attracting mass. Because the distances between the mercury pools and the attracting lead mass are large, the effect is very small. The mercury surface of the tilt meter pool is always vertical to the acceleration vector consisting of the earth gravity $\bar{g}$ and the mass attraction $\bar{A}$ of the lead assembly. The tangent to the surface in pool number 1 has an angle α_1 to the horizontal plane and the tangent to the surface in pool number 2 has an angle α_2 (Fig. C-1). The vectors A_1 and A_2 have x- and y-components.

$$\tan \alpha_1 = \frac{A_{1x}}{g + A_{1y}}$$

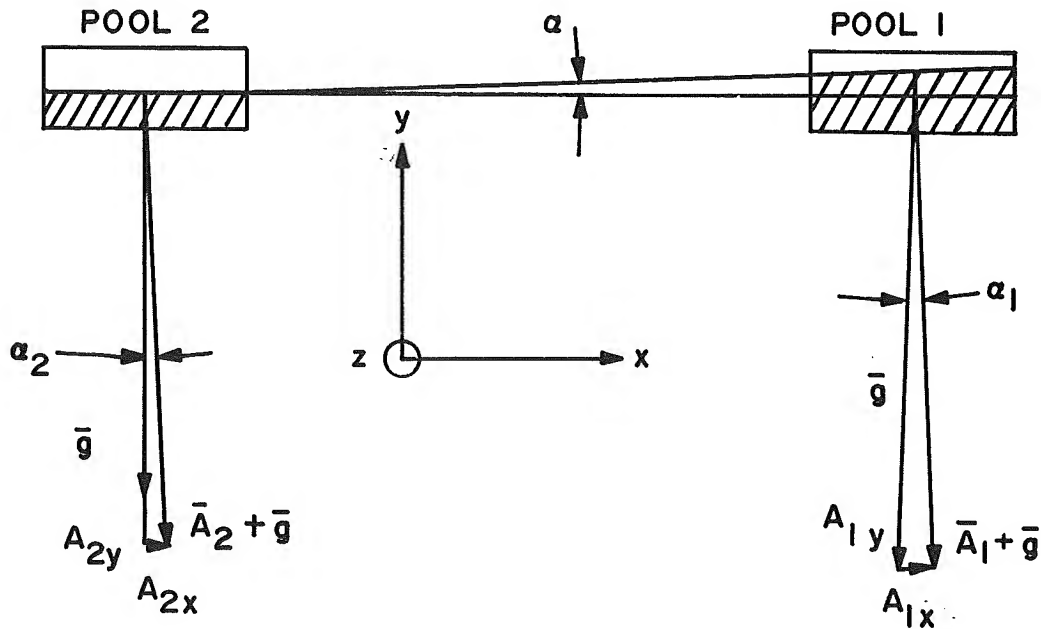$$\tan \alpha_2 = \frac{A_{2x}}{g + A_{2y}} \ .$$

Figure C-1. Mass attraction of the mercury in the tilt meter.

Since α_1, α_2, A_{1y}, and A_{2y} are very small,

$$\alpha_1 = \frac{A_{1x}}{g}$$

and

$$\alpha_2 = \frac{A_{2x}}{g} \quad .$$

A good approximation of the imaginary equipotential surface is a sphere. The line connecting the two pools is the secant line of the circle which is the intersection curve of the sphere with the x-y plane. The angle α between the secant line and the x-axis is the geometrical correlation

$$\alpha = \frac{1}{2}(\alpha_1 + \alpha_2) \text{ rad.}$$

This angle α is the output value of the tilt meter; α was computed for the three positions of the attracting mass.

Position up $\alpha_u = 0.680 \times 10^{-8}$ rad

Position middle $\alpha_m = 0.595 \times 10^{-8}$ rad

Position down $\alpha_d = 0.496 \times 10^{-8}$ rad .

The values also agree with those computed according to the potential theory. The movement of the mass causes a tilting of the mercury surface. The input tilting is almost a sine wave with the amplitude of $\alpha_A = 0.1 \pm 0.07 \times 10^{-8}$ rad.

The data analysis of the tilt meter data AY(I) shows an amplitude at the frequency FO of

$$BY(25) = (0.3 \pm 0.2) \ 10^{-8} \text{ rad.}$$

The value has a large standard deviation and is in the same magnitude as the computed amplitude for mass attraction. Therefore, no tilting of the test pad connected with the movement of the attracting mass was large enough to influence the calibration of the MESA in the laboratory.
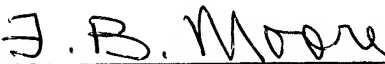
REFERENCES

1. Ganssle, E. R.: Gravity Gradiometry Mission Feasibility Study. NASA CR-24.3, Neotec Corp., Dec. 5, 1967.

2. Muller, P. M.; and Sjogren, W. L.: Mascons: Lunar Mass Concentrations. Science, vol. 161, no. 3842, Aug. 16, 1968, pp. 680-684.

3. Plourde, H. S.; and Nelson, R. H., Jr.: Low Level Accelerometer Test Methods. Dynamic Research Corp., E-578, June 30, 1965.

4. Macke, Wilhelm: Mechanik der Teilchen, Systeme und Kontinua. Akademische Verlagsgesellschaft (Leipzig), 1962.

5. McMillan, William Duncan: The Theory of the Potential. Dover Publications, 1958.

6. Meldrum, M. A.; Harrison, E. J.; and Milburn, Z.: Development of a Miniature Electrostatic Accelerometer (MESA) for Low g Applications. Summary Report, Bell Aerospace Co., Apr. 30, 1965.

7. Ideal Aerosmith: Tilt Meter Instructions.

8. Newberry, Murl. H.: Random Vibration Analysis Program (RAVAN). NASA TM X-53359, Nov. 17, 1965.

9. Bendat, Julius S.; and Piersol, Allan G.: Measurement and Analysis of Random Data. John Wiley and Sons, Inc., Feb. 1967.

10. Linnik, Yu V.: Method of Least Squares and Principle of the Theory of Observation. Pergamon Press, 1961.

APPROVAL

ACCELEROMETER CALIBRATION
IN THE LOW g RANGE
BY MEANS OF MASS ATTRACTION

By Konrad Reinel [1]

The information in this report has been reviewed for security classification. Review of any information concerning Department of Defense or Atomic Energy Commission programs has been made by the MSFC Security Classification Officer. This report, in its entirety, has been determined to be unclassified.

This document has also been reviewed and approved for technical accuracy.

F. B. MOORE
Director, Astrionics Laboratory

[1] National Research Council - NASA resident research associate on leave from the Institute for Dynamics of Flight Systems, DFVLR, Oberphaffenhofem, Germany

INTERNAL

DIR
DEP-T

PD-DO-DIR
  Dr. Thomason

S&E-CSE-DIR
  Dr. Haeussermann

S&E-ASTR-DIR
  Mr. Moore

S&E-ASTR-A
  Mr. Hosenthien
  Miss Flowers

S&E-ASTR-C
  Mr. Swearingen

S&E-ASTR-E
  Mr. Aden

S&E-ASTR-G
  Mr. Mandel
  Dr. Doane
  Mr. Broussard
  Mr. Fikes
  Mr. Walls   (20)
  Mrs. Neighbors

S&E-ASTR-I
  Mr. Duggan

S&E-ASTR-M
  Mr. Boehm

S&E-ASTR-R
  Mr. Taylor

S&E-ASTR-S
  Mr. Wojtalik

S&E-ASTR-ZX
A&TS-MS-IP   (2)
A&TS-MS-IL   (8)
A&TS-MS-H
AD-S
PM-PR-M

A&TS-PAT
  Mr. Wofford

A&TS-TU

EXTERNAL

Scientific and Technical Information
  Facility (25)
P.O. Box 33
College Park, Maryland 20740
Attn: NASA Representative
  (S-AK/RKT)

Dr. Jaenke
Holloman Air Force Base, N.M.

Dr. Knausentserger
Headquarters of Aerospace Research
Washington, D.C. 20036

Dr. Stieler
NASA Electronics Research Center
575 Technology Square
Cambridge, Mass. 02139

Mr. Lane
Bell Aerosystems
Buffalo, New York 14240